

Seismic Assessment of Steel Frames Subjected to Multi-hazards

Oualid Badla

Civil Engineering Department

Faculty of Technology

University of Khenchela

Khenchela, Algeria

badla.oualid@univ-khenchela.dz

Received: 3 September 2022 | Revised: 13 September 2022 | Accepted: 21 September 2022

Abstract-This paper investigates the effects induced by thunderstorm downbursts to steel building structures that have been previously damaged during strong directivity ground motion events. To achieve this objective, one four-story steel moment-resisting frame that was tested at the E-defense laboratory, Japan was analyzed in the nonlinear range using OpenSees. The seismic response was numerically simulated, obtaining a satisfactory agreement with the experimental evidence, revealing that the effects of such wind events and vertical ground motions were significant. These effects should be addressed during the design of low and medium buildings subjected to initial damage and subsequent thunderstorm downbursts and the ductility demands on structures subjected to multi-hazards can be quantified. The wind loads are applied as an externally applied dynamic load and the revised ductility demands are determined directly. The obtained results are compared to what is expected by experimental tests.

Keywords-steel building; thunderstorm downbursts; ductility demands; wind; earthquake; non-linear analysis

I. INTRODUCTION

The devastating effects of severe thunderstorms observed over the last decade have inspired researchers to study this complex phenomenon [1, 2]. Actual evidence shows that buildings damaged by earlier hazards are prone to secondary effects from consecutive multi-hazards, such as thunderstorm downbursts [3, 4]. This can increase damage after a disaster, eventually leading to the collapse of structures left unprotected after the primary hazards. A thunderstorm downburst differs from synoptic winds as it produces a small-scale follow-up divergence within a 5km radius, accompanied by intense microbursts. This configuration can cause damage corresponding to a synoptic wind sequence of 70m/s within a time interval of 5 to 20min [5, 6]. Due to the nose shape profile with different heights above the ground, the wind speed reaches its peak between 30 and 100m above the ground [7]. This phenomenon poses risks related to the collapse mechanism of low to high buildings [8, 9] There are still important knowledge gaps ranging from the design aspects to the evolution of contingency plans and strategies to increase resilience. The current guidelines have such limitations because they ignore

the co-occurrence of natural events such as earthquakes and winds [10-12]. A design framework that takes into account seismic loading and strong synoptic wind has recently been proposed [13]. Other studies focused on dealing with multi-hazards are [14, 15], although no studies have been conducted to determine the ductility requirements of damaged structures under additional effects of thunderstorm downbursts.

This paper investigates the seismic response and the effects of the downburst outflow wind at mean speeds ranging between 33m/s and 75m/s on the ductility of damaged buildings. The proposed methodology combines the principles of nonlinear static adaptive pushover analysis [16], which aims to reproduce the damage caused by the primary hazard event, and the sequential dynamic analysis [17-23], aiming to estimate the damage caused by the secondary sequential thunderstorm event.

II. CONSIDERED STEEL FRAME

A. Tested Bare Frame

The tested steel frame is described in [24-26] and only a brief explanation is given here. The test specimen consists of a 2-span 4-story moment-resistant steel frame shown in Figure 1. The two span-lengths in the main direction are 5m, while in the transversal direction the span-length is 6m. The heights of the ground floor and of the upper floors are 3.875m and 3.5m respectively. The ground floor columns are rigidly connected to 1.5m high load-bearing concrete blocks. The blocks, in turn, are clamped into the shaking table. The beam-column connections are inherently rigid and, following the practice developed after the 1995 Hyogoken-Nanbu earthquake, were detailed to force the formation of plastic hinges from the joints.

B. Description of the E-defense Experiments

The experiments consisted of shaking the sample frame with 3 scaled 3-D versions of the ground motion recorded in Takatori during the Kobe earthquake. The inputs were scaled at 40%, 60%, and 100%. The 40% input aimed to create only elastic deformations in the frame, the 60% input created inelastic deformations and nearly collapsed the frame, and the 100% input caused the frame to collapse.

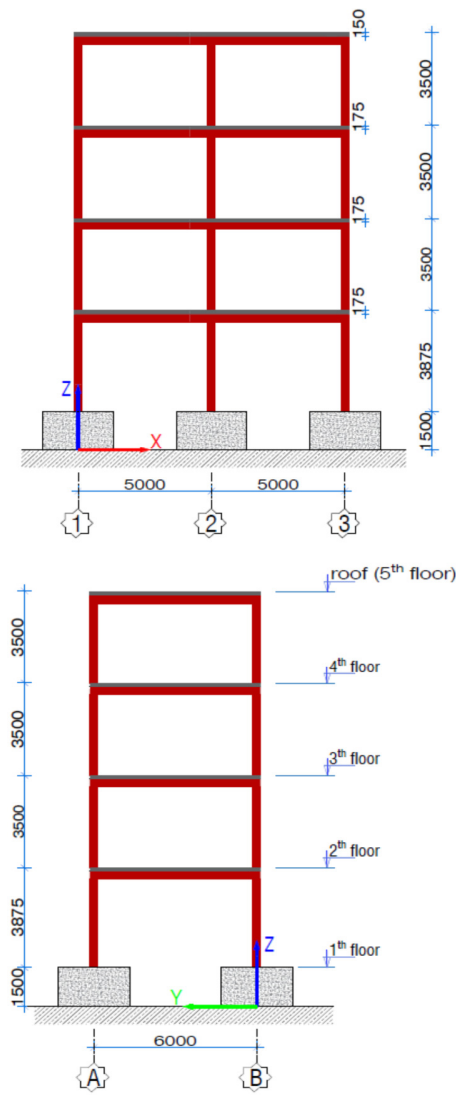


Fig. 1. Tested steel frame

III. EARTHQUAKE GROUND MOTIONS

The earthquake records used in this investigation are the horizontal and vertical components of the Newhall records from the 1994 Northridge earthquake, available from the Pacific Earthquake Engineering Research (PEER) center [27] (Figure 2). The record represents a range of severe ground motions and exhibits a near-fault effect. It has been indicated [28] that the structural response depends primarily on the peak acceleration impulse in the ground motions and that the continued motion of lower amplitude has little effect on the maximal responses. The peak ground accelerations for the horizontal and vertical components are 0.578g and 0.537g respectively.

IV. WIND DATABASE RECORD

The present study created a wind recording database based on the simulation method reported in [29, 30] and on the algorithm proposed in [31]. The database was previously used to study the inelastic analysis of multi-degree of freedom

systems damaged by earthquakes posteriorly subjected to wind load [19]. The cross-spectral density of the turbulent fluctuation is taken into account in the simulation of the wind field. Therefore, the wind actions on the building frame borders have been integrated into the concentrated load acting on the supporting members of the structures. The there-second peak velocity time series at the height of maximum velocity, i.e. $Z_{U_{max}} = 10\text{m}, 50\text{m}, \text{ and } 75\text{m}$ above the ground, are illustrated in Figure 3. The maximum velocities, U_{max} , are 59, 70, and 78m/s for $Z_{U_{max}} = 10, 50, \text{ and } 75\text{m}$. This defines three different velocities along the height of the structure and thus affects the lateral load distribution and the energy absorption capacity of the structure.

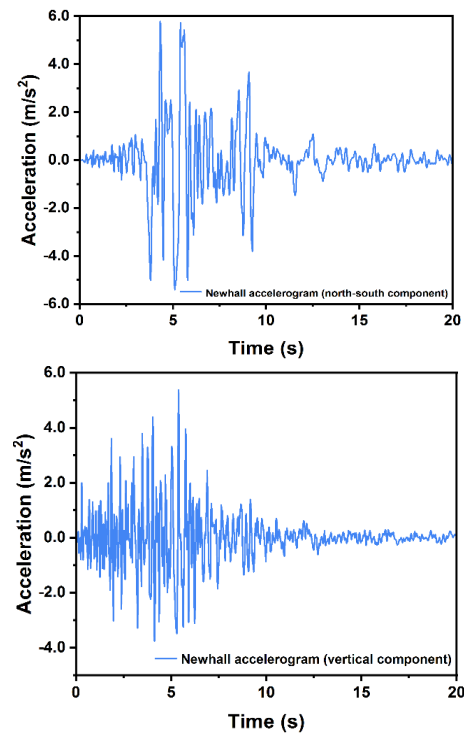


Fig. 2. Earthquake records.

The static forces induced by wind were calculated using (1).

$$F_i = \frac{1}{2} \rho C_D A_i U^2 \left(\frac{z}{z_r} \right)^{2\alpha} \quad (1)$$

where the reference height (z_r) was taken as 10m, ρ represents the air density, C_D is a drag coefficient, and A is the area exposed to the wind. Eurocode 1 gives values for α between 0.12 and 0.3, whilst a value of $\alpha = 0.22$ was used to represent the wind profile in suburban areas.

V. RESULTS AND DISCUSSION

A nonlinear static pushover analysis is initially presented to induce the ductility demand of the primary hazard events and identify the correlation between the base shear forces and the lateral roof displacement up to a target plastic deformation. The pushover analysis is used in order to bring the structure at a

pre-defined ductility demand level, including the descendant branch of the load-deformation curve, permitting direct control of the initially imposed damage. The transient non-stationary wind loads are subsequently applied as externally applied dynamic loads and the revised displacement ductility requirement is determined directly. Then, the ductility demands for different ductility levels can be calculated using (2):

$$\mu = \frac{d_{max}}{d_y} \quad (2)$$

where d_{max} is the target roof displacement, and $d_{yielding}$ is the corresponding yielding. The d_{max} is 0.04516, 0.05793, 0.1004, and 0.1828 for LD (Limited Damage), SD (Significant Damage), NC (Near Collapse), and CS (Collapse Start) damage states respectively, corresponding to roof displacement ductility. The yielding drift $d_{yielding}$ is 0.04516. The base shear force-roof displacement relationship of the considered steel frame is shown in Figure 4.

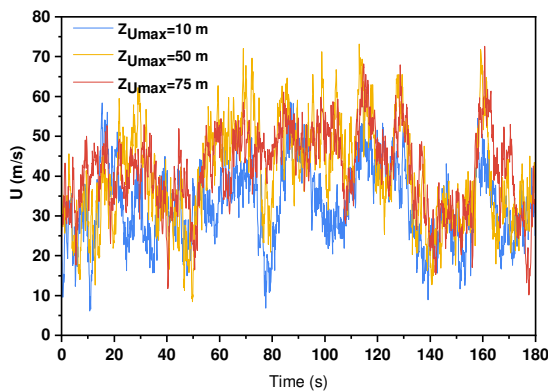


Fig. 3. Time history of the horizontal velocity at the height of the maximum velocity.

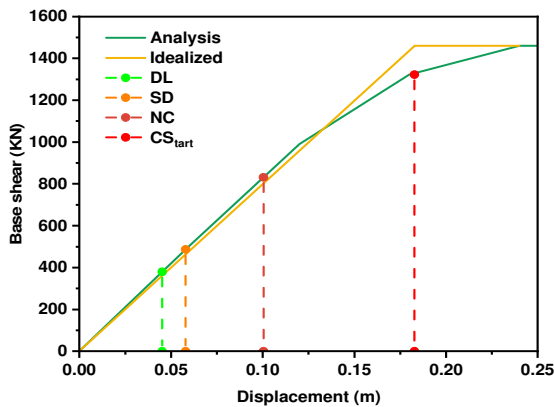


Fig. 4. Pushover capacity curves of considered steel frame.

Nonlinear analysis was carried out for different cases of the considered steel frame subjected to: (a) horizontal and vertical motions, (b) transient wind loads alone, and (c) to a combination of wind and both vertical and horizontal motions using the finite element program OpenSees [33].

Figures 5 and 6 show the comparison of the experimental results, the Pavan post-test results, and the numerical results of

displacements and shear forces at each floor. It is observed that once the actual input ground motion was considered in the analysis, the numerical predictions agreed relatively well with the experimental results.

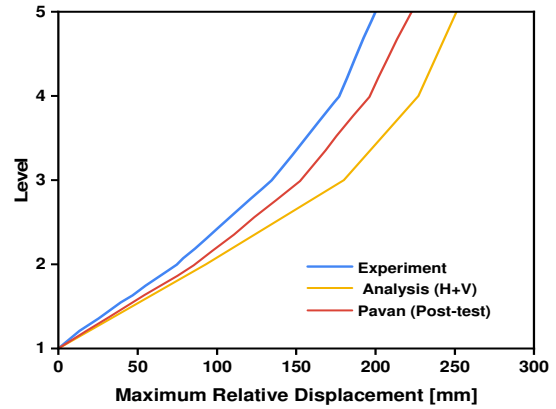


Fig. 5. Maximum relative displacement at every floor level.

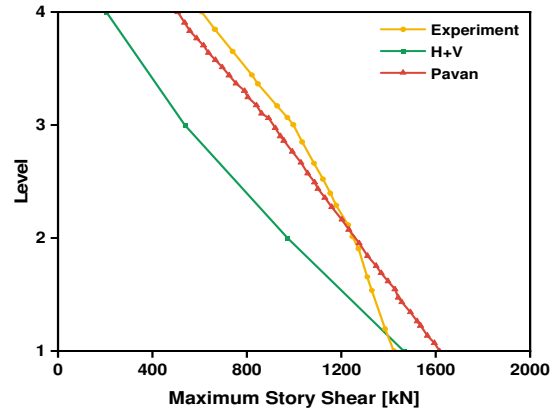


Fig. 6. Maximum story shear.

Initially, the transient wind loads (i.e. $Z_{Umax} = 10m$, $Z_{Umax} = 50m$, and $Z_{Umax} = 75m$) are applied on the steel frame alone and the results are shown in Figures 7 and 8. The deformations of the steel frame are within the elastic range under thunderstorm downburst for $Z_{Umax} = 10m$, since the ductility is less than 1, i.e. 0.61997 (Table I). Higher ductility can be observed under thunderstorm downburst, $Z_{Umax} = 50m$ and $75m$, as shown in Figure 7. The structural deformations entered to the plastic range and the maximum ductility demands are 1.26209 and 1.74921 respectively.

The base shear forces-roof displacement relationship for the sequential multi-hazards analysis is shown in Figures 9 and 10. The 3 simulated thunderstorm downburst scenarios are applied to the damaged steel frame which has previously attained a target ductility demand level (i.e. DL, SD, NC, and CS). The maximum ductility demands of the sequential analysis are summarized in Table I. This Table demonstrates, in general, that the ductility demands of the sequential wind event tend to increase as the initial target ductility level increases.

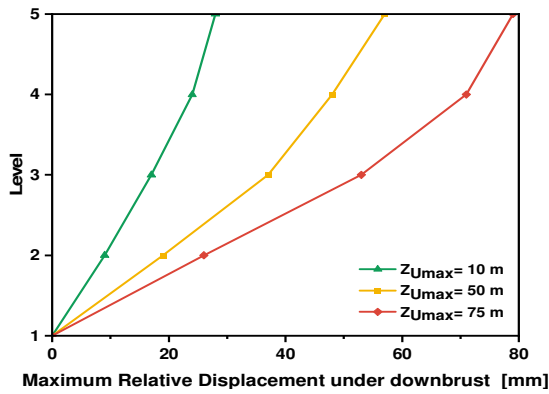


Fig. 7. Maximum relative displacement under downburst at every level.

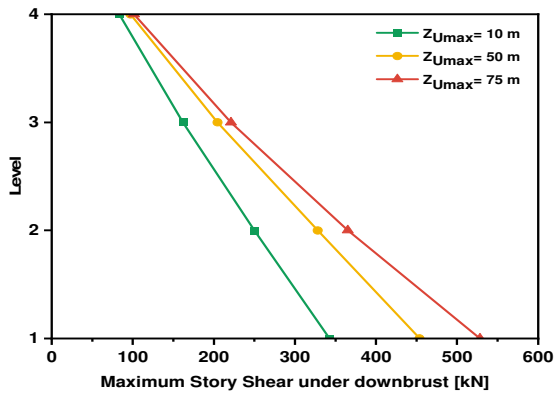


Fig. 8. Maximum story shear under downburst.

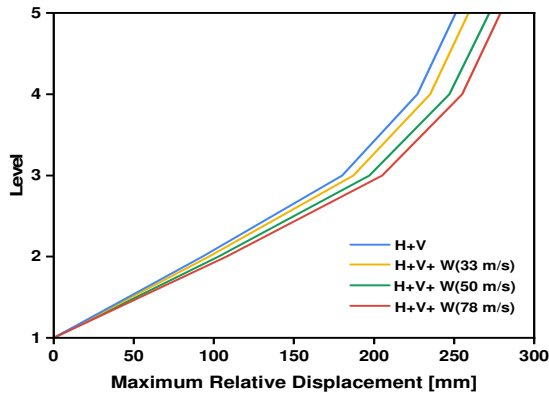


Fig. 9. Maximum relative displacement under multi-hazards at every level.

Under the sequential analysis of downburst outflow wind, the structure responded inelastically and higher plastic deformations than during the initial static pushover analysis were observed. The maximum ductility was found to be 5.73476, 6.02261, and 6.17760 respectively. The ductility demands increased significantly to 3.18725%, 8.36653%, and 11.15538% when the downburst reached the peak-velocity time series at the height of maximum velocity, i.e. Z_{Umax} = 10m, 50m and 75m above the ground than the ductility level of the primary event (simultaneous horizontal and vertical

excitations). Under these ductility demand levels, a collapse mechanism was formed.

The proposed approach can successfully identify the capacity limits and predict the failure mechanism of structures under sequential hazard events and can be implemented to appraise the increased ductility demands within a multi-hazard assessment framework.

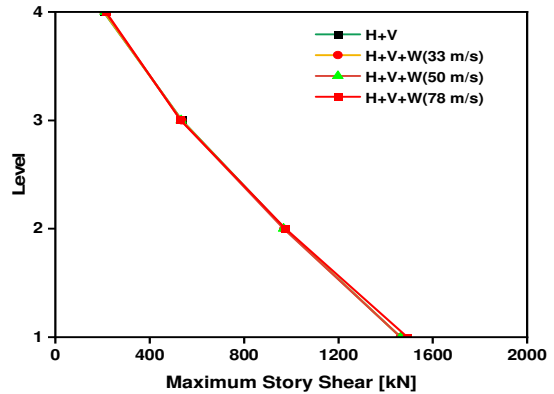


Fig. 10. Maximum story shear under multi-hazards.

TABLE I. DUCTILITY DEMAND FOR VARIOUS DOWNBURST SCENARIOS

Z_{Umax} (m)	10	50	75
Wind alone	0.61997	1.26209	1.74921
Limited Damage (DL)	5.73476	6.02261	6.17760
Significant Damage (SD)	4.47039	4.69477	4.81559
Near Collapse (NC)	2.57860	2.70803	2.77772
Collapse Start (CS)	1.41685	1.48796	1.52626

VI. CONCLUSIONS

The seismic behavior of steel frame structures under sequential hazard loads in the nonlinear range is investigated in the current paper. The main conclusions from the analysis can be summarized as follows:

- The input energy from the sequential downburst outflow wind event can push the structure into plasticity, exceeding the single hazard ductility demand. The damage level experienced by the structure during the secondary hazard event increases with the ductility demands of the primary event.
- Under the sequential analysis of downburst outflow wind, the ductility demand increases significantly by 3.18725%, 8.36653%, and 11.15538% from the ductility level of the primary event when the downburst reaches the peak-velocity time series at the height of maximum velocity of 10, 50, and 75m above the ground (simultaneous horizontal and vertical excitations).
- The proposed approach can successfully identify the capacity limits and predict the failure mechanism of structures under sequential hazard events and can be implemented to appraise the increased ductility demands within a multi-hazard assessment framework.

REFERENCES

- [1] H. E. Brooks, "Severe thunderstorms and climate change," *Atmospheric Research*, vol. 123, pp. 129–138, Apr. 2013, <https://doi.org/10.1016/j.atmosres.2012.04.002>.
- [2] A. T. Radler, P. H. Groenemeijer, E. Faust, R. Sausen, and T. Pucik, "Frequency of severe thunderstorms across Europe expected to increase in the 21st century due to rising instability," *npj Climate and Atmospheric Science*, vol. 2, no. 1, pp. 1–5, Aug. 2019, <https://doi.org/10.1038/s41612-019-0083-7>.
- [3] "Hurricane Katia leaves two dead in Mexico as earthquake clean-up begins," *ABC News*, Sep. 10, 2017. <https://www.abc.net.au/news/2017-09-10/deadly-quake-hurricane-katia-a-one-two-punch-for-mexico/>.
- [4] F. K. Narayan Chandrika, "Mexico had two major earthquakes this month. Here's why," *CNN*, Sep. 20, 2017. <https://www.cnn.com/2017/09/20/americas/mexico-two-earthquakes-in-one-month/index.html>.
- [5] T. T. Fujita, *The Downburst: Microburst and Macroburst*, 1st ed. Chicago, IL, USA: University of Chicago, 1985.
- [6] F. T. Lombardo, D. A. Smith, J. L. Schroeder, and K. C. Mehta, "Thunderstorm characteristics of importance to wind engineering," *Journal of Wind Engineering and Industrial Aerodynamics*, vol. 125, pp. 121–132, Feb. 2014, <https://doi.org/10.1016/j.jweia.2013.12.004>.
- [7] T. Theodore Fujita, "Downbursts: meteorological features and wind field characteristics," *Journal of Wind Engineering and Industrial Aerodynamics*, vol. 36, pp. 75–86, Jan. 1990, [https://doi.org/10.1016/0167-6105\(90\)90294-M](https://doi.org/10.1016/0167-6105(90)90294-M).
- [8] A. M. Loredou-Souza, E. G. Lima, M. B. Vallis, M. M. Rocha, A. R. Wittwer, and M. G. K. Oliveira, "Downburst related damages in Brazilian buildings: Are they avoidable?," *Journal of Wind Engineering and Industrial Aerodynamics*, vol. 185, pp. 33–40, Feb. 2019, <https://doi.org/10.1016/j.jweia.2018.11.022>.
- [9] A. Tilloy, B. D. Malamud, H. Winter, and A. Joly-Laugel, "A review of quantification methodologies for multi-hazard interrelationships," *Earth-Science Reviews*, vol. 196, Sep. 2019, Art. no. 102881, <https://doi.org/10.1016/j.earscirev.2019.102881>.
- [10] A. M. Aly and S. Abburu, "On the Design of High-Rise Buildings for Multihazard: Fundamental Differences between Wind and Earthquake Demand," *Shock and Vibration*, vol. 2015, Sep. 2015, Art. no. e148681, <https://doi.org/10.1155/2015/148681>.
- [11] D. Duthinh and E. Simiu, "Safety of Structures in Strong Winds and Earthquakes: Multihazard Considerations," *Journal of Structural Engineering*, vol. 136, no. 3, pp. 330–333, Mar. 2010, [https://doi.org/10.1061/\(ASCE\)ST.1943-541X.0000108](https://doi.org/10.1061/(ASCE)ST.1943-541X.0000108).
- [12] S. N. Thilakarathna, N. Anwar, P. Norachan, and F. A. Naja, "The Effect of Wind Loads on the Seismic Performance of Tall Buildings," *Athens Journal of Technology & Engineering*, vol. 5, no. 3, pp. 251–276, Aug. 2018, <https://doi.org/10.30958/ajte.5-3-3>.
- [13] S. Kwag, A. Gupta, J. Baugh, and H.-S. Kim, "Significance of multi-hazard risk in design of buildings under earthquake and wind loads," *Engineering Structures*, vol. 243, Sep. 2021, Art. no. 112623, <https://doi.org/10.1016/j.engstruct.2021.112623>.
- [14] S. Elias, R. Rupakhety, and S. Olafsson, "Analysis of a Benchmark Building Installed with Tuned Mass Dampers under Wind and Earthquake Loads," *Shock and Vibration*, vol. 2019, Nov. 2019, Art. no. e7091819, <https://doi.org/10.1155/2019/7091819>.
- [15] A. E. Taha, "Vibration Control of a Tall Benchmark Building under Wind and Earthquake Excitation," *Practice Periodical on Structural Design and Construction*, vol. 26, no. 2, May 2021, Art. no. 04021005, [https://doi.org/10.1061/\(ASCE\)SC.1943-5576.0000569](https://doi.org/10.1061/(ASCE)SC.1943-5576.0000569).
- [16] A. K. Chopra and R. K. Goel, "A modal pushover analysis procedure for estimating seismic demands for buildings," *Earthquake Engineering & Structural Dynamics*, vol. 31, no. 3, pp. 561–582, 2002, <https://doi.org/10.1002/eqe.144>.
- [17] D. Isobe and S. Tanaka, "Sequential Simulations of Steel Frame Buildings Under Multi-Phase Hazardous Loads During Earthquake and Tsunami," *Frontiers in Built Environment*, vol. 7, 2021, Art. no. 669601, <https://doi.org/10.3389/fbuil.2021.669601>.
- [18] Q. Li and B. R. Ellingwood, "Performance evaluation and damage assessment of steel frame buildings under main shock–aftershock earthquake sequences," *Earthquake Engineering & Structural Dynamics*, vol. 36, no. 3, pp. 405–427, 2007, <https://doi.org/10.1002/eqe.667>.
- [19] O. Badla, T. Bouzid, and P. M. Vazquez, "Inelastic Analysis of Mdf Systems Damaged by Earthquakes, Posteriorly Subjected to Wind Load," *Civil Engineering Journal*, vol. 7, no. 3, pp. 575–593, Mar. 2021, <https://doi.org/10.28991/cej-2021-03091675>.
- [20] S. Park, J. W. van de Lindt, D. Cox, R. Gupta, and F. Aguiniga, "Successive Earthquake-Tsunami Analysis to Develop Collapse Fragilities," *Journal of Earthquake Engineering*, vol. 16, no. 6, pp. 851–863, Aug. 2012, <https://doi.org/10.1080/13632469.2012.685209>.
- [21] R. A. Hakim, M. S. A. Alama, and S. A. Ashour, "Seismic Assessment of an RC Building Using Pushover Analysis," *Engineering, Technology & Applied Science Research*, vol. 4, no. 3, pp. 631–635, Jun. 2014, <https://doi.org/10.48084/etasr.428>.
- [22] H. Ullah, M. Rizwan, M. Fahad, and S. a. A. Shah, "Seismic Evaluation of the RC Moment Frame Structure using the Shake Table," *Engineering, Technology & Applied Science Research*, vol. 11, no. 1, pp. 6674–6679, Feb. 2021, <https://doi.org/10.48084/etasr.3959>.
- [23] P. C. Nguyen, "Nonlinear Inelastic Earthquake Analysis of 2D Steel Frames," *Engineering, Technology & Applied Science Research*, vol. 10, no. 6, pp. 6393–6398, Dec. 2020, <https://doi.org/10.48084/etasr.3855>.
- [24] M. Tada, M. Ohsaki, S. Yamada, S. Motoyui, and K. Kasai, "E-Defense Tests on Full-Scale Steel Buildings: Part 3 - Analytical Simulation of Collapse," in *Research Frontiers at Structures Congress 2007*, Jun. 2012, [https://doi.org/10.1061/40944\(249\)19](https://doi.org/10.1061/40944(249)19).
- [25] K. Suita, S. Yamada, M. Tada, K. Kasai, Y. Matsuoka, and Y. Shimada, "Collapse experiment on 4-story steel moment frame: Part 2 detail of collapse behavior," in *14th World Conference on Earthquake Engineering*, Beijing, China, Oct. 2008.
- [26] A. Pavan, R. Pinho, and S. Antoniou, "Blind prediction of a full scale 3D steel frame tested under dynamic conditions," in *14th World Conference on Earthquake Engineering*, Beijing, China, Oct. 2008.
- [27] "PEER Ground Motion Database - PEER Center." <https://ngawest2.berkeley.edu/#disclaimer>.
- [28] R. W. Clough and K. L. Benuska, "FHA Study of Seismic Design Criteria for High-Rise Buildings," Federal Housing Administration, Washington DC, USA, Report HUD TS-3, 1966.
- [29] P. Martinez-Vazquez and N. Rodriguez-Cuevas, "Wind field reproduction using neural networks and conditional simulation," *Engineering Structures*, vol. 29, no. 7, pp. 1442–1449, Jul. 2007, <https://doi.org/10.1016/j.engstruct.2006.08.024>.
- [30] P. Martinez-Vazquez, "Wind-induced vibrations of structures using design spectra," *International Journal of Advanced Structural Engineering*, vol. 8, no. 4, pp. 379–389, Dec. 2016, <https://doi.org/10.1007/s40091-016-0139-4>.
- [31] E. H. Vanmarcke, E. Heredia-Zavoni, and G. A. Fenton, "Conditional Simulation of Spatially Correlated Earthquake Ground Motion," *Journal of Engineering Mechanics*, vol. 119, no. 11, pp. 2333–2352, Nov. 1993, [https://doi.org/10.1061/\(ASCE\)0733-9399\(1993\)119:11\(2333\)](https://doi.org/10.1061/(ASCE)0733-9399(1993)119:11(2333)).
- [32] PEER, "Guidelines for Performance-Based Seismic Design of Tall Buildings," University of California, Berkeley, CA, USA, 2010/05, 2010.
- [33] "Open System for Earthquake Engineering Simulation - Home Page." <https://opensees.berkeley.edu>.